ELSEVIER

Engineering Analysis with Boundary Elements 25 (2001) 557–564

ENGINEERING ANALYSIS *with* BOUNDARY ELEMENTS

www.elsevier.com/locate/enganabound

A unified formulation and error estimation measure for the direct and the indirect boundary element methods in elasticity

M. Denda*, Y.F. Dong

Department of Mechanical and Aerospace Engineering, Rutgers University, 98 Brett Road, Piscataway, NJ 08854-8058, USA

Received 24 April 2000; revised 28 November 2000; accepted 15 January 2001

Abstract

In this paper, given a boundary value problem for a finite elastic body in two-dimensions, a problem of representing the solution by layers of point forces (F_j) and Somigliana dislocations (B_j) is considered in the infinite homogeneous body that contains the original finite body. In the boundary element method (BEM) solution, either the boundary displacement or traction component at each node is specified, but not both. This provides us a degree of freedom to arbitrarily specify the proportion of the densities F_j and B_j to be used in the direct and the indirect BEM formulations. The nature of the BEM solution errors is identified and a unified error estimation measure with a mesh refinement scheme for both formulations is proposed.

Keywords: Direct and indirect boundary element methods; Dislocation and point force approach; A posteriori error estimation; Unified error estimation measure

1. Introduction

Study on error estimation and mesh refinement processes is the key element in the pursuit of adaptive boundary element methods (BEMs) for potential and elastic problems as summarized in review papers [1,2]. These papers provide classifications of existing error estimation methods such as: the residual methods in the Galerkin BEM [3,4] and in the collocation BEM [4–6], the extrapolation error estimates [7–10], the projection error estimates [9,11], and the solution sensitivity based error estimates [12]. They also classify mesh refinement schemes in the BEM as: h-, p-, r-refinement schemes and the combination of them. Other important papers [13–15], are concerned with the use of the boundary integral equation (BIE) and the hypersingular boundary integral equation (HBIE) together for error estimation.

Among various formulations of the BEM in elasticity there exist the direct and the indirect formulations as discussed in literature [16–18]. While the direct boundary element method (DBEM) formulation is derived from Somigliana's identity [19,20], the indirect boundary element method (IBEM) formulation is given by the fictitious point force or Somigliana dislocation distribution [21–23]. Note that Somigliana dislocation is specified by a loop in 3-D and a dipole in 2-D. Traditionally, these two formulations have been developed independently. However, a physical interpretation [24–27] of Somigliana's identity can relate the DBEM and the IBEM by means of the point force and Somigliana dislocation distributions and delineates important characteristics of the BEM. Denda and Dong [27] has applied this physical interpretation and proposed an error estimation measure, for the direct BEM, based on the external Somigliana's identity. The present paper extends Denda and Dong's work [27] to provide a unified formulation and error estimation scheme for the direct and the indirect BEM formulations as summarized next.

Given a boundary value problem for a finite elastic body, a problem of representing the solution by layers of point forces (F_j) and Somigliana dislocations (B_j) is considered, in Section 2, in the infinite homogeneous body that contains the original finite body. In the BEM solution, either the boundary displacement or traction component at each node is specified, but not both as discussed in Section 3. This provides us a degree of freedom to arbitrarily specify the proportion of the densities F_j and B_j to be used in the direct and the indirect BEM formulations. For example, the selection of $B_j = 0$ will lead to an indirect formulation in terms of the point force distribution, while $F_j = 0$ will give another indirect formulation by Somigliana dislocation distribution, as described in Section 4.2. It is also possible to use nonzero densities of F_j and B_j in an arbitrary proportion to propose multitudes of indirect formulations.

* Corresponding author. Tel.: +1-732-445-4391; fax: +1-732-445-3124.
E-mail address: denda@jove.rutgers.edu (M. Denda).

0955-7997/01/$ - see front matter
PII: S0955-7997(01)00017-0

Selection of B_j to be the boundary displacement, as in Section 4.1, will give the direct formulation and F_j is shown to be given by the boundary traction. Finally, in Section 5, the nature of the BEM solution errors in the direct and the indirect formulations is identified and a unified error estimation measure with a mesh refinement scheme for both formulations is proposed.

2. Point force and Somigliana dislocation solutions in the infinite domain

In the infinite domain, the singular displacement solution for a point force $f_j(\xi)$ at ξ is given by

$$u_k^{(f)}(z) = G_{kj}(z, \xi) f_j(\xi), \tag{1}$$

where $G_{kj}(z,\xi)$ is the Green's tensor function [16,17], representing the displacement in the x_k direction at z due to the unit point force in the x_j direction at ξ. The subscripts vary from 1 to 3 in 3-D and 1 to 2 in 2-D, respectively. From Eq. (1), the stress and the traction over a surface with the unit outward normal n_j at z are derived as

$$\sigma_{mk}^{(f)}(z) = \sigma_{mkj}(z, \xi) f_j(\xi), \tag{2}$$

$$t_k^{(f)}(z) = P_{kj}(z, \xi) f_j(\xi), \tag{3}$$

where

$$\sigma_{mkj}(z, \xi) = C_{mkil} \frac{\partial G_{ij}(z, \xi)}{\partial z_l}, \qquad P_{kj}(z, \xi) = n_m \sigma_{mkj}(z, \xi), \tag{4}$$

and C_{ijkl} is the stiffness constants. Notice that the term surface is used both in 3-D and in 2-D, the latter actually being a line. The functions $\sigma_{mkj}(z,\xi)$ and $P_{kj}(z,\xi)$ represent the stress σ_{mk} and the traction t_k at z, respectively, due to the unit point force in the x_j direction at ξ.

For a point force distribution with the density $F_j(\xi)$ on a smooth surface S, the displacement and the stress at a point z are obtained by integrating expressions (1) and (2) over the surface with the result

$$u_k(z) = \int_S G_{kj}(z, \xi) F_j(\xi)\, \mathrm{d}S, \tag{5}$$

$$\sigma_{mk}(z) = \int_S \sigma_{mkj}(z, \xi) F_j(\xi)\, \mathrm{d}S. \tag{6}$$

The traction over a surface at z with the unit outward normal n_j is given by

$$t_k(z) = \int_S P_{kj}(z, \xi) F_j(\xi)\, \mathrm{d}S. \tag{7}$$

When the point z approaches the surface S, the tractions calculated on the two sides of the surface S are different. Let $\tilde{n}_j$ be the unit outward normal of the surface S and define the positive side $S^{(+)}$ and the negative side $S^{(-)}$ of the surface S, as shown in Fig. 1; when crossing the surface S in the direction $\tilde{n}_j$ one moves from $S^{(+)}$ to $S^{(-)}$. Fig. 1 also shows the outward normals of $S^{(+)}$ and $S^{(-)}$ defined by $\tilde{n}_j$ and $-\tilde{n}_j$. The variables indicated by the superscripts $(+)$ and $(-)$ represent their limiting values from the positive and the negative sides, respectively. This convention of positive and negative sides of a surface will be used throughout this paper. It is verified that the displacement is continuous but that the traction undergoes a jump across S as summarized by the relations

$$u_j^{(+)}(\xi) - u_j^{(-)}(\xi) = 0, \quad t_j^{(+)}(\xi) + t_j^{(-)}(\xi) = F_j(\xi), \qquad \xi \in S, \tag{8}$$

where the lower case letters u and t, with superscripts $(+)$ and $(-)$, are used for the limit displacement and traction, respectively.

Consider another fundamental solution due to the Somigliana dislocation, i.e. the dislocation loop in 3-D and the dislocation dipole in 2-D, in the infinite domain. A dislocation loop/dipole over the surface S shown in Fig. 1 is defined by a displacement jump of magnitude $B_j(\xi)$ identified as the Burgers vector but the traction is continuous,

$$t_j^{(+)}(\xi) + t_j^{(-)}(\xi) = 0, \quad u_j^{(+)}(\xi) - u_j^{(-)}(\xi) = B_j(\xi), \qquad \xi \in S. \tag{9}$$

Once again the term surface is used for 3-D and 2-D. The displacement solution due to the Somigliana dislocation distribution $B_j(\xi)$ is given by [28]

$$u_k(z) = \int_S Q_{kj}(z, \xi) B_j(\xi)\, \mathrm{d}S, \tag{10}$$

with

$$Q_{kj}(z, \xi) = -C_{mjil} \frac{\partial G_{ik}(z, \xi)}{\partial \xi_l} \tilde{n}_m, \tag{11}$$

where $\tilde{n}_j$ is the unit normal of the surface S as shown in Fig. 1. The function $Q_{kj}(z,\xi)$ represents the displacement in the x_k direction at z due to the unit displacement jump in the x_j direction over unit area on the infinitesimal surface $\mathrm{d}S$ at ξ. It is related to $P_{jk}(\xi,z)$ by

$$Q_{kj}(z, \xi) = -P_{jk}(\xi, z), \tag{12}$$

by selecting $n_j = \tilde{n}_j$ for $P_{jk}(\xi, z)$. The stress and the traction

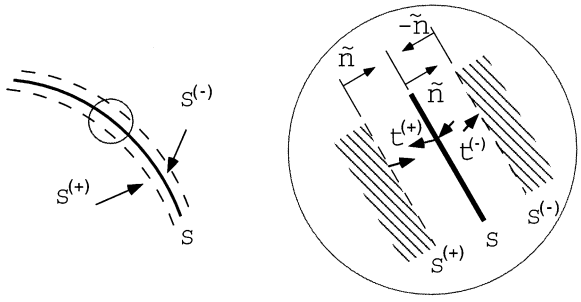

Fig. 1. Definition of the positive and the negative sides of a surface.

over a surface with the unit normal n_j at z are given by

$$\sigma_{mk}(z) = \int_S S_{mkj}(z, \xi) B_j(\xi)\, \mathrm{d}S, \tag{13}$$

$$t_k(z) = \int_S D_{kj}(z, \xi) B_j(\xi)\, \mathrm{d}S, \tag{14}$$

where $S_{mkj}(z,\xi)$ and $D_{kj}(z,\xi)$ represent the stress σ_{mk} and the traction t_k at z, respectively, due to the unit displacement jump in the x_j direction at ξ. The solutions given in Eqs. (10), (12) and (13) are continuous in the infinite domain except the displacement discontinuity across the surface S, as the condition (9) states.

Consider a hypothetical problem given by the point force and the Somigliana dislocation distributions over a set of surfaces in the infinite domain. The elastic solution at a point z is given by the superposition of all contributions from these distributions. The point force and Somigliana dislocation distributions give rise to the traction and the displacement discontinuities, respectively, across their surfaces. Accordingly, when a surface S is subject to both the point force and Somigliana dislocation distributions, the superposition of Eqs. (8) and (9) will give the jumps in the displacement and traction across this surface,

$$u_j^{(+)}(\xi) - u_j^{(-)}(\xi) = B_j(\xi), \quad t_j^{(+)}(\xi) + t_j^{(-)}(\xi) = F_j(\xi), \quad \xi \in S. \tag{15}$$

3. Infinite domain representation of finite domain problems

Let V represent a finite region enclosed by the boundary ∂V as shown in Fig. 2(a). The boundary ∂V is subject to the displacement $U_j(\xi)$ and the traction $T_j(\xi)$. Of course, only the displacement or traction component in a given direction, at each boundary node, is prescribed in a well-posed boundary value problem. The solution of this finite domain problem can be represented by the point force and Somigliana dislocation distributions in the infinite body of the same material, as described below.

Let us divide the infinite domain into two parts: the region $V^{(+)} = V$ that coincides with the finite body considered and its complementary region $V^{(-)}$ separated by the surface $S = \partial V$, as shown in Fig. 2(b). The unit outward normal $\tilde{n}_j$ of the boundary ∂V points from $S^{(+)}$ to $S^{(-)}$. On the surface S place distributions of point forces and Somigliana dislocations with densities $F_j(\xi)$ and $B_j(\xi)$, respectively. The resulting displacement, stress and traction at any point z in the infinite body, either in $V^{(+)}$ or $V^{(-)}$, are given by

$$u_k(z) = \int_S G_{kj}(z, \xi) F_j(\xi)\, \mathrm{d}S + \int_S Q_{kj}(z, \xi) B_j(\xi)\, \mathrm{d}S, \tag{16}$$

$$\sigma_{mk}(z) = \int_S \sigma_{mkj}(z, \xi) F_j(\xi)\, \mathrm{d}S + \int_S S_{mkj}(z, \xi) B_j(\xi)\, \mathrm{d}S, \tag{17}$$

$$t_k(z) = \int_S P_{kj}(z, \xi) F_j(\xi)\, \mathrm{d}S + \int_S D_{kj}(z, \xi) B_j(\xi)\, \mathrm{d}S. \tag{18}$$

The densities $B_j(\xi)$ and $F_j(\xi)$ are determined such that the displacement and the stress in $V^{(+)}$ agree with the solution for the original finite body V.

When the point z approaches S from the region $V^{(+)}$ the limit values $u_k^{(+)}(\xi)$ and $t_k^{(+)}(\xi)$ of the displacement and traction, respectively, is obtained from Eqs. (16) and (18). In the following, it is proved that the necessary and sufficient condition for the infinite domain problem to actually represent the solution to the original finite body is given by:

$$u_k^{(+)}(\xi) = U_k(\xi), \qquad \xi \in S. \tag{19}$$

This condition ensures that the limit value of the displacement $u_k^{(+)}(\xi)$ agrees with the boundary displacement $U_k(\xi)$ on the boundary ∂V of the original finite body. To prove the above claim make a cut along the surface $S^{(+)}$ on

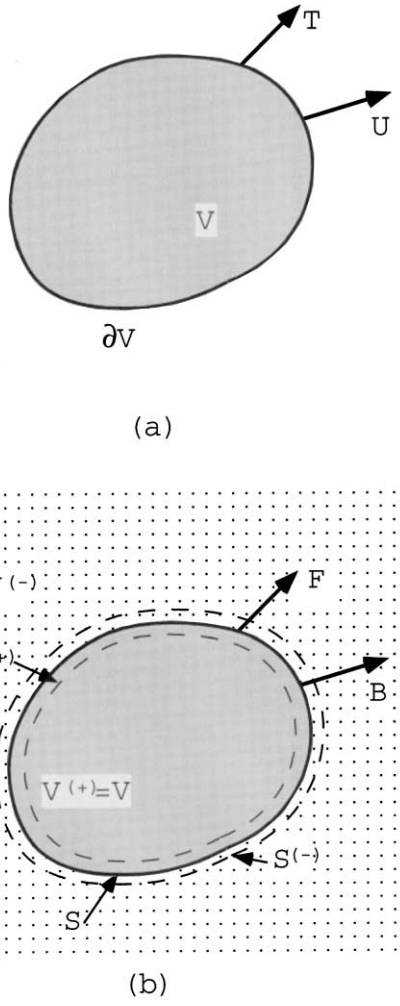

Fig. 2. (a) A finite body problem and (b) the corresponding infinite body problem.

the positive side and remove the region $V^{(+)}$ out of the infinite domain keeping the same deformation as it is embedded in the infinite domain. This will lead to a new boundary value problem for $V^{(+)}$ which has the same geometry and the boundary displacement as the original finite body as shown in Fig. 2(a). This implies that the solutions (16)–(18) given in the region $V^{(+)}$ agree with those for the original finite body. Consequently, the limit value of the traction $t_k^{(+)}(\xi)$ agrees with the boundary traction $T_k(\xi)$ on the boundary ∂V of the real problem,

$$t_k^{(+)}(\xi) = T_k(\xi), \qquad \xi \in S. \tag{20}$$

Alternatively, it is proved that if the condition (20) is satisfied, then the deformation in the region $V^{(+)}$ is the same as in the original finite body and the Eq. (19) holds except for an arbitrary rigid body displacement. Therefore, the Eq. (20), instead of Eq. (19), becomes the necessary and sufficient condition for the infinite domain problem to actually represent the solution to the original finite body. In summary, the Eqs. (19) and (20) can be viewed as constraints upon the two density functions $B_j(\xi)$ and $F_j(\xi)$. Since one equation is satisfied automatically as a consequence of the other, they give only one independent constraint on $B_j(\xi)$ and $F_j(\xi)$. As a result, another constraint can be imposed by specifying either $B_j(\xi)$ or $F_j(\xi)$ arbitrarily at each point on the surface S. It is this freedom of specification for the values of $B_j(\xi)$ and $F_j(\xi)$ that yields a variety of different BEM formulations as demonstrated in the Section 4.

4. Different versions of the boundary element method

4.1. Direct boundary element method

To derive the DBEM formulation, set the magnitude $B_j(\xi)$ of Somigliana dislocation in Eqs. (16)–(18) as

$$B_j(\xi) = U_j(\xi), \tag{21}$$

which is the boundary displacement of the finite domain problem. This choice of $B_j(\xi)$, with Eqs. (9) and (19), will lead to

$$u_j^{(-)}(\xi) = u_j^{(+)}(\xi) - B_j(\xi) = 0, \qquad x \in S, \tag{22}$$

on $S^{(-)}$, which sets a zero displacement boundary condition for the region $V^{(-)}$. The solution of this boundary value problem is given by the zero displacement and stress, i.e.

$$u_k(z) = 0, \quad \sigma_{kj}(z) = 0, \qquad z \in V^{(-)}, \tag{23}$$

in the region $V^{(-)}$ implying the condition

$$t_j^{(-)}(\xi) = 0, \tag{24}$$

on its boundary $S^{(-)}$. The last Eq. (24), with Eqs. (20) and (8), determines the value of $F_j(\xi)$ according to

$$F_j(\xi) = t_j^{(+)}(\xi) = T_j(\xi), \qquad \xi \in S. \tag{25}$$

In conclusion, the magnitudes of $B_j(\xi)$ and $F_j(\xi)$ are given by the boundary displacement and the traction, respectively, of the finite domain problem. The displacement and traction for the point z in $V^{(+)}$ of the infinite domain problem are given by

$$u_k(z) = \int_S G_{kj}(z,\xi)T_j(\xi)\,\mathrm{d}S + \int_S Q_{kj}(z,\xi)U_j(\xi)\,\mathrm{d}S, \tag{26}$$

$$t_k(z) = \int_S P_{kj}(z,\xi)T_j(\xi)\,\mathrm{d}S + \int_S D_{kj}(z,\xi)U_j(\xi)\,\mathrm{d}S, \tag{27}$$

which also give the solution of the finite domain problem. The solution of the infinite domain problem in the region $V^{(-)}$ is zero. When the point z approaches S from the region V, i.e. $V^{(+)}$, the Eqs. (26) and (27) together with the condition (19) or (20) yield the DBEM formulations: the displacement formulation with the BIE and the traction formulation with the HBIE, respectively.

Using the symmetry conditions,

$$G_{kj}(z,\xi) = G_{kj}(\xi,z) = G_{jk}(\xi,z),$$

and (12), Eq. (26) can be rewritten as

$$u_k(z) = \int_S G_{jk}(\xi,z)T_j(\xi)\,\mathrm{d}S - \int_S P_{jk}(\xi,z)U_j(\xi)\,\mathrm{d}S. \tag{28}$$

This is the standard form of Somigliana identity for the DBEM obtainable from the Betti–Rayleigh reciprocal theorem through the use of the point force solution.

4.2. Indirect boundary element method

An IBEM can be obtained by setting the value of $B_j(\xi)$ to zero on the whole surface S,

$$B_j(\xi) = 0. \tag{29}$$

The displacement and traction for both the finite domain problem and its corresponding infinite domain problem are given, according to Eqs. (16) and (18), by

$$u_k(z) = \int_S G_{kj}(z,\xi)F_j(\xi)\,\mathrm{d}S, \tag{30}$$

$$t_k(z) = \int_S P_{kj}(z,\xi)F_j(\xi)\,\mathrm{d}S. \tag{31}$$

When the point z approaches S from the region V, Eqs. (30) and (31) together with the condition (19) or (20) yields an IBEM formulation.

Since one of the magnitudes of $B_j(\xi)$ and $F_j(\xi)$ at each point on the surface S can be arbitrarily specified, different formulations of the IBEM can be obtained by specifying $B_j(\xi)$ and $F_j(\xi)$ on the surface S differently. For example, it is possible to specify $F_j(\xi) = 0$ on some part of the surface S and $B_j(\xi) = 0$ on the rest of surface S and a BEM formulation is obtained from Eqs. (16) and (18) by applying the condition (19) or (20).

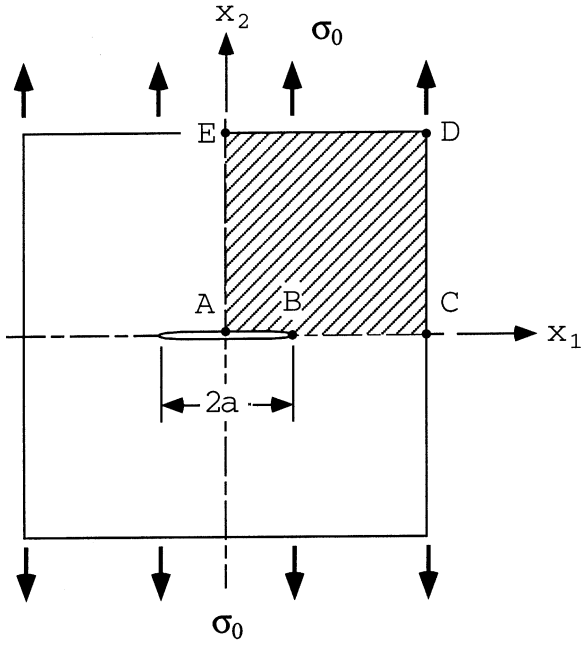

Fig. 3. A centre crack in a large plate under tension.

5. Unified error estimation

As shown in Section 4, the formulations of the direct and the indirect BEM are based on the condition (19) or (20), necessary and sufficient for the infinite domain problem to represent the finite domain problem, and an arbitrary selection of the values of $F_j(\xi)$and $B_j(\xi)$. In the implementation of the collocation BEM, the surface S is discretized into elements $S = \sum_e S_e$ and approximate, in each element, the boundary values $U_j(\xi)$ and $T_j(\xi)$, using the interpolations $\tilde{U}_j(\xi)$ and $\tilde{T}_j(\xi)$, which are given in terms of the boundary values at collocation points. (Note that in the DBEM these interpolations $\tilde{U}_j$(x) and $\tilde{T}_j(\xi)$ also serve as the density functions in the integral representations (26) and (27). In the IBEM it is necessary to introduce an additional interpolation for the density function $F_j(\xi)$ for the integral representations (30) and (31).) The limit values $u_k^{(+)}(\xi)$ and $t_k^{(+)}(\xi)$, which appear on the left hand sides of the Eqs. (19) and (20), are calculated from Eq. (26) for the displacement formulation and Eq. (27) for the traction formulation of the DBEM and from Eqs. (30) and (31) for the IBEM with $B_j(\xi) = 0$. In the numerical analysis in general these limit values $u_k^{(+)}(\xi)$ and $t_k^{(+)}(\xi)$ do not agree with those given by the interpolations $\tilde{U}_k(\xi)$ and $\tilde{T}_k(\xi)$ on the surface S. Thus

$$u_k^{(+)}(\xi) - \tilde{U}_k(\xi) \neq 0, \qquad t_k^{(+)}(\xi) - \tilde{T}_k(\xi) \neq 0, \tag{32}$$

on the boundary except possibly at some, but not all, of the collocation points. In the DBEM either the traction or the displacement mismatch indicated by Eq. (32) always exist. In the displacement formulation of the DBEM that uses Eq. (26) the displacement $u_k^{(+)}(\xi)$, but not the traction, on the positive side of the boundary is forced to match the displacement $\tilde{U}_k(\xi)$ at collocation points; as a consequence it is seen that $u_k^{(+)}(\xi) - \tilde{U}_k(\xi) = 0$ but $t_k^{(+)}(\xi) - \tilde{T}_k(\xi) \neq 0$. In the traction formulation that uses Eq. (27), on the other hand, the traction $t_k^{(+)}(\xi)$, instead of the displacement, on the positive side of the boundary is forced to match the traction $\tilde{T}_k(\xi)$ so that it is observed that $t_k^{(+)}(\xi) - \tilde{T}_k(\xi) = 0$ but $u_k^{(+)}(\xi) - \tilde{U}_k(\xi) \neq 0$. Whether the displacement or the traction matches at a given collocation point depends solely on the formulation (i.e. the displacement or the traction DBEM) but not on the boundary condition there. In the IBEM, on the other hand, both the displacement and the traction are forced to match the corresponding boundary values, i.e. $u_k^{(+)}(\xi) - \tilde{U}_k(\xi) = 0$ and $t_k^{(+)}(\xi) - \tilde{T}_k(\xi) = 0$, at each collocation point.

To measure the difference between the interpolated boundary values and the limit values along the whole boundary surface S, define the following residual functions:

$$R_k^{(u)}(\xi) = \tilde{U}_k(\xi) - u_k^{(+)}(\xi), \tag{33}$$

$$R_k^{(t)}(\xi) = \tilde{T}_k(\xi) - t_k^{(+)}(\xi). \tag{34}$$

The norms of these displacement and traction residual

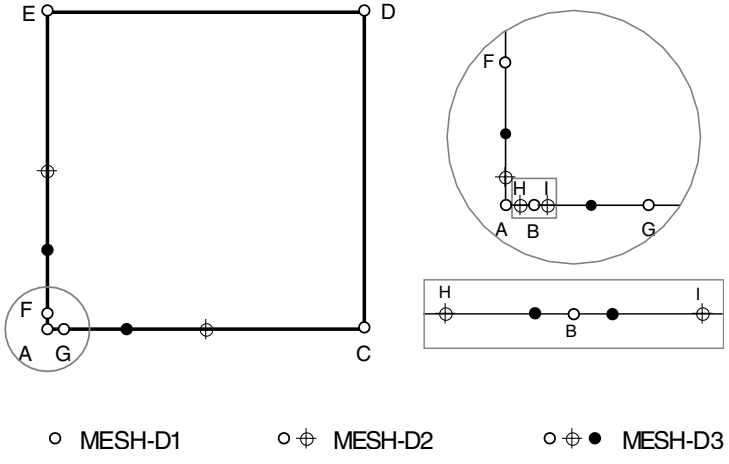

Fig. 4. Meshes for the DBEM.

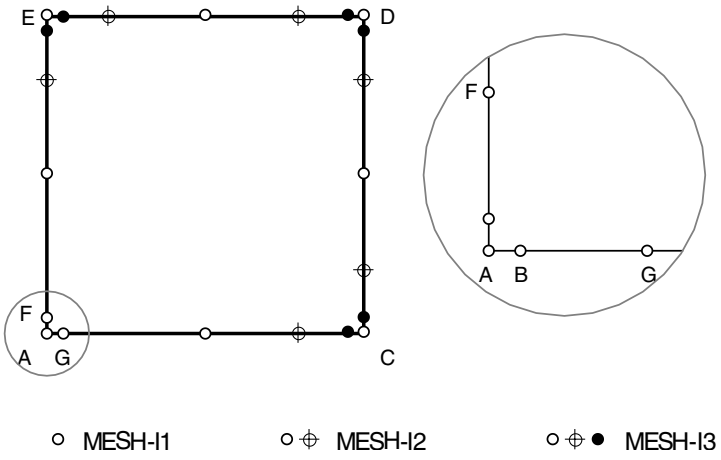

Fig. 5. Meshes for the IBEM.

functions are given by

$$\|R^{(u)}\| = \int_S R_j^{(u)} R_j^{(u)} \mathrm{d}S \qquad \text{and} \qquad \|R^{(t)}\| = \int_S R_j^{(t)} R_j^{(t)} \mathrm{d}S, \tag{35}$$

which may be used for the error estimation in the DBEM and the IBEM. The difference in the units of $\|R^{(u)}\|$ and $\|R^{(t)}\|$, however, prevents us from simply adding them to get an error indicator. Instead, define the error indicator by

$$W^{(R)} = \sqrt{\|R^{(u)}\| \, \|R^{(t)}\|}, \tag{36}$$

which has the unit of energy. The error indicator for an individual element S_e will be defined by

$$W_e^{(R)} = \sqrt{\int_{S_e} R_j^{(u)} R_j^{(u)} \mathrm{d}S \int_{S_e} R_j^{(t)} R_j^{(t)} \mathrm{d}S}, \tag{37}$$

which is the residual over the element.

In the adaptive mesh refinement of the DBEM and IBEM, it is suggested to refine the elements by subdividing the elements with high values of both the error indicator $W_e^{(R)}$ and the element mean error indicator $W_{em}^{(R)} = W_e^{(R)}/A_e$, where A_e is the area or arc length of the element S_e in 3-D and 2-D, respectively.

Denda and Dong [27] have developed another error indicator for the DBEM, which is based on the strain energy in the region $V^{(-)}$ complementary to $V^{(+)}$ in the infinite body. A conversion of the volume integral over $V^{(-)}$ to a surface integral leads to an error indicator

$$W^{(-)} = \int_S [u_k^{(+)}(\xi) - \tilde{U}_k(\xi)][\tilde{T}_k(\xi) - t_k^{(+)}(\xi)] \, \mathrm{d}S$$

$$= -\int_S R_k^{(u)}(\xi) R_k^t(\xi) \, \mathrm{d}S, \tag{38}$$

where the integration is defined over the boundary S of the finite body V with its unit normal pointing away from V.

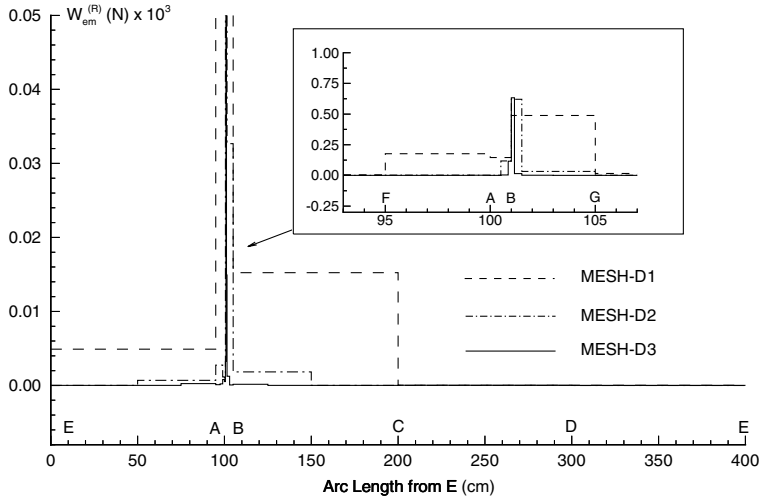

Fig. 6. The element mean error distribution $W_{em}^{(R)}$ of the DBEM solution.

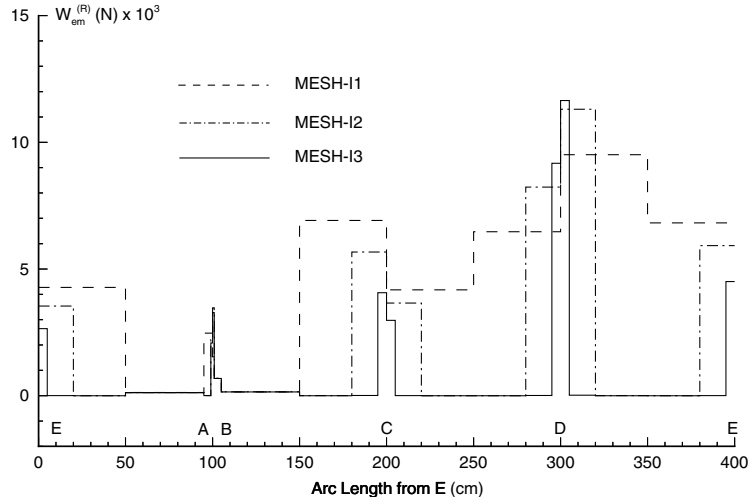

Fig. 7. The element mean error distribution $W_{\mathrm{em}}^{(R)}$ of the IBEM solution.

6. Numerical example

Using both the displacement formulation of the DBEM and the IBEM with $B_j(\xi) = 0$, a center crack problem in the two dimensional infinite medium subject to the uniaxial remote tension $\sigma_0 = 1$ MPa in x_2 direction is investigated; continuous elements are used. Analytical formulas for the BEM (Denda and Dong [27]), obtained by evaluating integrals analytically using the straight element, are used to minimize the numerical error. Plane strain condition is considered with Poisson's ratio $\nu = 0.3$ and the shear modulus $\mu = 10^5$ MPa. Exploiting the symmetry, the problem is analyzed by modeling only one quarter of a large plate 200×200 cm (2×2 m) containing a crack ($a = 1$ cm), as shown in Fig. 3.

Fig. 4 shows three meshes used for the displacement formulation of the DBEM: Mesh-D1, Mesh-D2 and Mesh-D3, and Fig. 5 shows three meshes used for the IBEM with $B_j(\xi) = 0$: Mesh-I1, Mesh-I2 and Mesh-I3. Although the quadratic interpolation functions are employed, only the end nodes of the elements are shown in Figs. 4 and 5. Subdividing some elements of Mesh-D1 by adding new end nodes forms Mesh-D2, based on which Mesh-D3 is constructed by adding more new end nodes. Following the same procedure, Mesh-I2 is generated from Mesh-I1 and Mesh-I3 from Mesh-I2. Only those elements which have large values of $W_{\mathrm{e}}^{(R)}$ and $W_{\mathrm{em}}^{(R)}$ are subdivided.

Shown in Figs. 6 and 7 are the element mean error distributions $W_{\mathrm{em}}^{(R)}$ for the DBEM and the IBEM. The abscissa in these two figures is the arc length measured from the point E in the direction toward A, C, D and back to E. Five sample points on each element are used to interpolate the residual functions $R_j^{(u)}$ and $R_j^{(t)}$; use of more than five sample points did not change the results significantly. It is found that while the errors near the crack surface dominate in the DBEM, the errors near the corners of the boundary are dominant in the IBEM; the reason for this is under investigation. Tables 1 and 2 show the reduction in the values of the global error indicator as the mesh is refined. With the help of error indicator, rapid convergence of the numerical solution is achieved for both the DBEM and the IBEM. The results also show less error in the DBEM than in the IBEM for the crack problem considered.

7. Concluding remarks

In this paper, the necessary and sufficient condition for the infinite domain problem, defined in Section 2, to represent the solution for the finite domain is identified. This condition provides a degree of freedom to specify the magnitude of one of the density functions $B_j(\xi)$ and $F_j(\xi)$ arbitrarily, which is the basis for the various BEM formulations. A unified error indicator for both the DBEM and the IBEM based on the boundary integrals of the displacement and the traction residual functions over each element is proposed, following the observation on the nature of the BEM errors. The element error indicator serves as an error

Table 1
Global error estimation $W^{(R)}$ (Nm) of DBEM

Meshes	Mesh-D1	Mesh-D2	Mesh-D3
Elements	7	12	18
$W^{(R)} \times 10^4$	1.33618	0.22985	0.05761

Table 2
Global error estimation $W^{(R)}$ (Nm) of IBEM

Meshes	Mesh-I1	Mesh-I2	Mesh-I3
Elements	11	18	24
$W^{(R)} \times 10^2$	2.02555	0.84393	0.23720

measure for each element and is used in the adaptive mesh refinement scheme. The numerical example has demonstrated the effectiveness of the proposed error indicator and the adaptive mesh refinement strategy.

Acknowledgements

This work was supported by the FAA Center for Computational Modeling of Aircraft Structures at Rutgers University.

References

[1] Kita E, Kamiya N. Recent studies on adaptive boundary element methods. Adv Engng Software 1994;19:21–32.
[2] Liapis S. Error estimation and adaptivity in boundary element methods. In: Atluri SN, Yagawa G, Cruse TA, editors. Computational mechanics '95, 2. New York: Springer, 1995. p. 2659–64.
[3] Hsiao GC, Kleinman RE. Feasible error estimates in boundary element methods. In: Brebbia CA, Ingber MS, editors. Boundary element technology, vol. VII. Southampton: Computational Mechanics Publication, 1992. p. 875–86.
[4] Rank E. Adaptive boundary element methods. In: Brebbia CA, Wendland WL, Kuhn G, editors. Boundary elements, vol. IX. Southampton: Computational Mechanics Publication, 1987. p. 259–78.
[5] Parreira P, Dong YF. Adaptive hierarchical boundary elements. Adv Engng Software 1992;15:249–59.
[6] Rank E. Adaptive h-, p- and hp- versions for boundary integral element methods. Int J Numer Meth Engng 1989;28:1335–49.
[7] Charafi A, Wrobel LC, Adey R. An approach to h-adaptive boundary element method using local reanalysis. In: Brebbia CA, Ingber MS, editors. Boundary element technology, vol. VII. Southampton: Computational Mechanics Publication, 1992. p. 90–918.
[8] Kita E, Kamiya N. A new adaptive boundary element refinement based on simple algorithm. Mech Res Commun 1991;18:177–86.
[9] Rencis JJ, Jong KY. A self-adaptive h-refinement technique for the boundary element method. Comput Meth Appl Mech Engng 1989;73:295–316.
[10] Rencis JJ, Mullen RL. Solution of elasticity problems by a self-adaptive mesh refinement technique for boundary element computation. Int J Numer Meth Engng 1986;23:1509–27.
[11] Rencis JJ, Hopkins DA, Chamis CC. Local and global accuracy estimate for boundary element method. Finite Elem Analys Design 1991;9:229–45.
[12] Guiggiani M. Error indicators for adaptive mesh refinement in the boundary element method. Int J Numer Meth Engng 1990;29:1247–69.
[13] Paulino GH, Gray LJ, Zarikian V. Hypersingular residuals — a new approach for error estimation in the boundary element method. Int J Numer Meth Engng 1996;39:2005–29.
[14] Menon G, Paulino GH, Mukherjee S. Analysis of hypersingular residual error estimates in boundary element methods for potential problems. Comput Meth Appl Mech Engng 1999;173:449–73.
[15] Liang MT, Chen JT, Yang SS. Error estimation for boundary element method. Engng Analys Boundary Elem 1999;23:257–65.
[16] Banerjee PK, Butterfield R. Boundary element methods in engineering science. London: McGraw-Hill, 1981.
[17] Brebbia CA, Telles JCF, Wrobel LC. Boundary element techniques: theory and applications in engineering. New York: Springer, 1984.
[18] Jaswon MA, Symm GT. Integral equation methods in potential theory and elastostatics. London: Academic Press, 1977.
[19] Rizzo FL. An integral equation approach to boundary value problems of classical elastostatics. Quart Appl Math 1967;25:83–95.
[20] Cruse TA. Numerical solutions in three-dimensional elastostatics. Int J Solids Struct 1969;5:1259–74.
[21] Massonnet CE. Numerical use of integral procedures. In: Zienkiewicz OC, Holister GS, editors. Stress analysis – recent developments in numerical and experimental methods. New York: Wiley, 1965. p. 198–235.
[22] Oliviera ERA. Plane stress analysis by a general integral method. J Engng Mech Div ASCE 1968;94:79–85.
[23] Banerjee PK. Integral equation methods for analysis of piece wise non-homogeneous three-dimensional elastic solids of arbitrary shape. Int J Mech Sci 1976;18:293–303.
[24] Eshelby JD. The elastic field of a crack extending non-uniformly under general anti-plane loading. J Mech Phys Solids 1969;17:177–99.
[25] Altiero NL, Gavazza SD. On a unified boundary-integral equation method. J Elasticity 1980;10(1):1–9.
[26] Denda M, Dong YF. Complex variable approach to the BEM for multiple crack problems. Comput Meth Appl Mech Engng 1997;141:247–64.
[27] Denda M, Dong YF. An error estimation measure in the direct BEM formulation by the external Somigliana's identity. Comput Meth Appl Mech Engng 1999;173:433–47.
[28] Mura T. Micromechanics of defects in solids. 2nd ed. Dordrecht: Martinus Nijhoff, 1987.